

Intracranial calcifications on CT: an updated review

Charbel Saade¹, Elie Najem², Karl Asmar², Rida Salman², Bassam El Achkar², Lena Naffaa^{2*}

1. Department of Medical Imaging Sciences, American University of Beirut Medical Center, Beirut, Lebanon

2. Department of Diagnostic Radiology, American University of Beirut Medical Center, Beirut, Lebanon

* **Correspondence:** Lena Naffaa, MD, Address: Diagnostic Radiology Department, American University of Beirut Medical Center, PO Box: 11-0236, Riad El Solh, Beirut 1107 2020, Beirut, Lebanon
(✉ ln01@aub.edu.lb)

Radiology Case. 2019 Aug; 13(8):1-18 :: DOI: 10.3941/jrcr.v13i8.3633

ABSTRACT

Intracranial calcifications are frequently encountered in non-contrast computed tomography scan in both adult and pediatric age groups. They refer to calcifications within the brain parenchyma or vasculature and can be classified into several major categories: physiologic/age-related, dystrophic, congenital disorders/phakomatoses, infectious, vascular, neoplastic, metabolic/endocrine, inflammatory and toxic diseases. In this updated review, we present a wide spectrum of intracranial calcifications from both pediatric and adult populations focusing on their pattern, size and location.

REVIEW ARTICLE

REVIEW ARTICLE

Introduction

Intracranial calcifications refer to calcifications within the brain parenchyma or vasculature (1). Their prevalence ranges from 1% in young individuals to up to 20% in elderly. However, brain calcifications were reported in up to 72% in autopsy cases with microscopic calcifications being the most common (2).

The usage of Computed Tomography scans has largely contributed in the accurate detection, localization and classification of intracranial calcifications (3). Even with the introduction of Magnetic Resonance Imaging in the 1990s, CT scan yet proved to be superior in the detection and characterization of brain calcifications. IC include physiologic/age-related calcifications and a wide spectrum of pathological calcifications (2). Nonetheless, previous studies were successful in linking various IC based on their radiological phenotype to specific pathological conditions such as vascular calcifications in stroke patients and basal ganglia calcifications in patients with hypoparathyroidism (1).

In this review, we present a wide array of intracranial calcifications (*Table 1 & 2*) with a particular focus on their appearance, size and location in order to formulate a better clinical approach of IC (*Figure 1*).

Physiologic/Age-Related Intracranial Calcifications

Physiologic calcifications are usually incidental findings on NCCT scan and tend to be more prevalent in older age groups.

They are usually found in the pineal gland, choroid plexus, habenula, falx cerebri and tentorium cerebelli (4,5). In a study that was done by Yalcin et.al that focused on determining the location and extent of IC in 11,941 subjects, the pineal gland was found to be the most common site of physiologic calcifications (71.6%) followed by the choroid plexus (70.2%) with male dominance in both sites with a mean age of 47.3 and 49.8 respectively. However, the choroid plexus was found to be the most common site of physiologic calcification after the 5th decade and second most common after the pineal gland in subjects aged between 15-45 years (3). In another study done by Whitehead et.al on 500 pediatric subjects, a total of 40% (202/500 study subjects) were found

to have physiologic calcifications with 97% being older than 5 years of age. Interestingly, calcifications were found to be more common in the choroid plexus (58/500) followed by the habenula (50/500) and pineal gland (25/500) (5).

Pineal calcifications are usually described as coarse and compact (6) (Fig. 2a and 2b). According to Whitehead et.al, pineal calcifications were punctate and single in all patients younger than 7 years of age and were occasionally found to be larger and numerous in patients older than 7. Hence, this observation should warrant careful examination and further investigations in patients younger than 7 years with relatively large or more numerous pineal calcifications (5). Other studies postulate that calcifications greater than 1 cm or found in patients younger than 9 years of age should warrant further investigations as they may point towards underlying neoplasms (4, 6). Thus, suspicious calcifications should be further investigated with a glandular volume assessment and clinical and biochemical investigations.

Choroid plexus calcifications are usually found in the atria of the lateral ventricles and are less common in the third and fourth ventricles or in patients younger than 9 years (6) (Fig. 2c and 2d). According to Whitehead et. al, all choroid plexus calcifications that were detected in children were found in the lateral ventricles as well and appeared mostly punctate (5). However, atypical locations of the choroid plexus calcifications such as at the level glomerula, bodies of the lateral ventricles, roof of the third ventricle and foramina of Monro should raise suspicion of an underlying pathology (4).

Habenular calcifications often exhibit a curvilinear pattern few millimeters anterior to the pineal body in up to 15% of adults (4, 6). The habenula is structurally connected to several deep areas of the brain hence serving as a relay and processing center influencing dopamine and serotonin elaboration. Thus, habenular calcifications were noted as frequent findings in schizophrenic patients (5).

According to Yalcin et.al, dural calcifications were seen in up to 12.5% of the studied population with the majority found in male patients. Subjects with dural calcifications were older than those with pineal, choroid or habenular calcifications with a mean age of 53.1. Of note, choroid plexus calcifications were concomitantly seen in up to 78.4% of patients with dural calcifications (3). However, according to whitehead et.al, dural calcifications were present in only 1% of the studied population with an age range between 2.9 – 8.7 years. Calcifications were mostly seen in the tentorium followed by the falx cerebri (5) (Fig. 2e).

Basal ganglia calcifications were found in only 1.3% in the same study conducted by Yalcin et.al. Interestingly, BGC were reported to be more prevalent among females than males with a mean age of 52.4. The prevalence of basal ganglia calcifications did not change with increased age. The majority of BGC was seen in the globus pallidus and was concurrently seen with pineal calcifications in up to 82.6% of the cases (3) (Fig. 2f).

Genetic / Developmental Disorders:

Intracranial calcifications are common findings in neurocutaneous syndromes. They are mostly seen in Sturge-Weber syndrome and tuberous sclerosis. However, they are less common in other phakomatoses such as neurofibromatosis and Cockayne syndrome (CS) (4, 6).

Sturge-Weber syndrome (SWS), also known as encephalotrigeminal angiomas, is a sporadic neurocutaneous syndrome characterized by a facial port wine stain, ipsilateral leptomeningeal vascular malformation and intracranial calcifications. Common neurological symptoms include seizures, hemiparesis, visual field defects and mental retardation (7, 8). Intracranial calcifications are usually detected using NCCT scan exhibiting a tram track appearance, a double-lined gyriform pattern that are parallel to the cerebral convolutions. Calcifications are thought to arise from cortical or subcortical ischemia secondary to pial angiomas (1). However, IC may not be seen during the first year of life and may even remain undetectable until few more years (8) (Fig. 3a).

Tuberous sclerosis is an autosomal dominant disease causing hamartomas in the brain, kidneys, skin and other organs.

Neuroimaging reveal subependymal hamartomas, subcortical tubers, giant cell tumors and white matter lesions. IC calcifications are seen in up to 54% of patients with TS and are more prevalent in older age groups with calcified subcortical tubers being more common in elderly. Calcifications of the subependymal nodules are pathognomonic and are usually located along the caudothalamic groove and atrium (6, 9) (Fig. 3b).

Neurofibromatosis is a heterogeneous group of hereditary cancer syndromes that lead to the formation of tumors of the central and peripheral nervous systems with neurofibromatosis type 1 (NF1) being more common than neurofibromatosis type 2 (NF2). Tumors associated with NF1 include peripheral nerve sheath tumors, gliomas, leukemia, pheochromocytomas and gastrointestinal stromal tumors. NF2 is characterized by the development of schwannomas, meningiomas, ependymomas, and ocular abnormalities (10). Intracranial calcifications are caused by calcium deposition in hamartomatous glial proliferations similarly to TS (1, 4). The most common non-tumoral calcifications are often described as symmetrical or asymmetrical of the choroid plexus of the lateral ventricles and nodular calcifications of the cerebellum. On the other hand, the most common calcifications in NF2 are usually associated with underlying tumors, often meningiomas (4) (Fig. 3c).

Cockayne syndrome is an autosomal recessive disorder characterized by cachectic dwarfism, shriveled and wrinkled skin, loss of subcutaneous fat, beaked nose, stooped posture with some patients exhibiting severe photosensitivity. CS is often associated with brain calcifications and are often seen in patients older than 3 years of age. Calcifications are unfrequently seen in patients younger than 1 year of age even in severe cases (11). Calcifications are often bilateral rock or

spot calcifications at the level of the basal ganglia with or without gyral calcifications. Cerebellar, dentate, thalamic, and leptomeningeal calcifications have been described as well to a lesser extent (1, 11) (*Fig. 3d*).

Krabbe disease is an autosomal recessive disorder characterized by early clinical symptoms before 4 months of age.

Symptoms include irritability, hypersensitivity to stimulation, startle response, spasticity, poor feeding, unexplained recurrent high fever and microcephaly (12). Brain calcifications are noted at the level of the internal capsule and corona radiata in areas of abnormal white matter and globoid cells accumulation (1) (*Fig. 3e*)

Aicardi-Goutières Syndrome is an autosomal recessive disorder that presents either during neonatal or infantile period. The neonatal form presents as fever, seizures, hepatosplenomegaly, thrombocytopenia, anemia with or without microcephaly. However, the infantile form presents as irritability, fever, loss of skills and acquired microcephaly. Brain calcification associated with AGS has been described as symmetrical, spot-like calcification at the level of the basal ganglia and deep white matter of both frontal and parietal lobes. Other sites have been implicated as well and include the dentate, cerebellar cortex, brainstem and deep and superficial cerebral cortex (1) (*Fig. 3f*)

Fahr disease is a rare neurodegenerative condition with more than 35 different names used in publications including bilateral striopallidodentate calcification and idiopathic basal ganglia calcification. Indeed, Fahr disease exhibits a wide range of clinical presentations ranging from asymptomatic to severe movement and neuropsychological disorders (1,13). IC in Fahr disease usually involve the grey matter structures and to less extent the white matter. They are typically described as symmetrical, involving the caudate, putamen, globus pallidus, thalamus, deep cortex and dentate (1) (*Fig. 3g*).

Congenital/Acquired Infections:

Congenital:

Cytomegalovirus infection is the most common among the TORCH infection with a prevalence ranging from 0.6-0.7% in industrialized countries. Congenital CMV infection is caused by transplacental transmission following a primary or secondary maternal infection (14). Congenital CMV infection is usually associated with chorioretinitis, microcephaly and IC (6). IC are the most common findings and are seen in 34-70% of congenital CMV infections. They tend to be associated with developmental delay and strongly implicate mental retardation compared to other radiological findings. Calcifications are usually seen in the periventricular area, brain parenchyma or basal ganglia. Periventricular calcifications are usually described as thick and chunky in appearance whereas calcifications in the basal ganglia are usually faint and punctate (14) (*Fig. 4a*).

Neonatal Herpes is the second most common TORCH infection after CMV with a prevalence of 1 in 5,000 and 80% fatality rate. Congenital infection occurs through perinatal

transmission of Herpes Simplex Virus 2 from cutaneous lesions (14) leading to extensive cerebral damage, multicystic encephalomalacia and scattered calcifications (6).

Congenital toxoplasmosis is caused by transplacental transmission of *Toxoplasma gondii* with an incidence of 0.1 – 0.6%. The infection rate varies throughout the pregnancy with the lowest infection rate being 20% in the first trimester and the highest in the third trimester scoring up to 60% (14). Congenital infection is generally associated with hydrocephalus and IC (4, 6, 14). Calcifications are nodular in shape in the periventricular area and cortex whereas they are curvilinear in the thalamus and basal ganglia (4) with larger calcifications being associated with earlier infections (14). According to a study done by Patel et. al, congenital toxoplasmosis calcifications tend to decrease or may even resolve after treatment. In fact, out of 56 infants with congenital toxoplasmosis, 75% of the treated infants experienced a decreased or even resolved calcifications whereas 25% had a stable examination (15) (*Fig. 4b*).

Congenital rubella infection has become rare and less prevalent with the introduction of the rubella vaccine. Congenital infection is transmitted transplacentally following a primary maternal infection leading to encephalitis, seizures, and cataracts, hearing loss, cardiac defects and IC (14). Calcifications are usually found at the level of the basal ganglia and periventricular area (6, 14).

Congenital Zika infection was first introduced in 2015 after an increase in the number of newborns with microcephaly in Pernambuco, Brazil. Nonetheless, Zika virus itself was first described in 1947 but no association between primary maternal Zika infection and microcephaly was made until 2015 in Brazil as previously mentioned. Primary infection occurs following a bite of an infected arthropod with a high risk of transmission via the placenta to the fetus in case of pregnancy leading to several neurological defects. According to a study done by Aragao et. al, IC were the main imaging findings on CT scans of 23 children diagnosed with congenital infection. Calcifications were mostly located between the cortex and subcortical white matter with punctate calcifications being the most common in addition to lesser linear and coarse calcifications (16).

Human Immunodeficiency Virus encephalitis can be both congenital or acquired (*Fig. 5*). Congenital infection is usually caused by a transplacental transmission leading to CNS invasion and myelin sheath damage. Neuroimaging may show microcephaly, ventriculomegaly, cerebral atrophy, and symmetrical IC in the basal ganglia and subcortical matter (14).

Acquired

Neurocysticercosis is a parasitic infection endemic in Mexico, South America, Asia and Africa. It is caused by the tapeworm *Taenia Solium* after the ingestion of undercooked meat. After ingestion, *Taenia Solium* migrates then to the CNS causing cerebral inflammation upon larvae death which shows as a ring enhancing lesion with adjacent edema (14). This is then followed by the development of a typical IC showing in

the brain parenchyma and subarachnoid space as an eccentric calcified nodule within a peripherally calcified cyst (4) (Fig. 6).

Mycobacterium tuberculosis infection primarily targets the respiratory system with the lungs being the major primary site. However, 5-10% of tuberculous infections involve the CNS either through the development of tuberculous meningitis or intracranial tuberculoma. Intracranial tuberculomas are usually encountered in both HIV-positive and immunocompetent individuals in endemic areas (17). Tuberculomas may then calcify in the center giving the appearance of a pathognomonic target sign with a surrounding ring enhancement with meningeal calcifications being less common (4) (Fig. 7a & 7b).

Cryptococcus neoformans infection affects primarily patients with advanced HIV infection and AIDS. Neuroradiological findings may vary according to the hematogenous spread of the fungus along the perivascular spaces at the base of the brain (18). Calcifications are usually rare findings and are seen late in the disease as punctate calcifications in the brain parenchyma and leptomeninges. Leptomeningeal calcifications specifically may represent sequelae of chronic subdural and epidural empyema (4, 18).

Vascular

Intracranial atherosclerosis is considered to be the most common cause of stroke worldwide. Vascular calcifications appear in up to 90% of atherosclerotic lesions and are considered as a potential predictor for ischemic strokes (19). In fact, they were noted in up to 82% of ischemic stroke patients and in 52% of non-ischemic stroke patients with an overall prevalence of 3.5%. The incidence of vascular calcifications is higher with increasing age and peaks in individuals older than 65 (3). Calcifications are seen in the wall of intracranial arteries, more frequent in the internal carotid (60%), vertebral (20%), middle cerebral (5%), and basilar arteries (5%) (20) (Fig. 8).

Vascular calcifications are also seen in cavernous angiomas (Fig. 9), arteriovenous malformations, dural arteriovenous fistulas and aneurysms. In cavernous angioma, they are seen in up to 33% of the cases (4). They are reported as scattered dots or stippled in the vessel wall or adjacent brain parenchyma, commonly in non-hemorrhagic lesions. Calcifications in venous angioma and capillary telangiectasias have been described scarcely. IC associated with AVM is seen in 25-30% mostly along the tortuous veins or the nidus or may be of dystrophic nature due to ischemic injury away from the malformation (21). Calcifications are also seen in AVFs showing a non-specific pattern of bilaterally symmetrical subcortical calcifications. Bilateral symmetrical subcortical calcifications may be seen as previously described in SWS, TS, and Fahr disease. However, unlike all the previously listed conditions, in AVFs no other foci of calcifications are noted (4). Calcifications that are associated with brain aneurysms are commonly seen in partially or completely thrombosed aneurysms and less frequently, in the wall of non-thrombosed aneurysms, preferentially fusiform versus saccular types (21, 22).

In the pediatric population, a spontaneous intimal tear or dissection may lead to the formation of an intracranial aneurysm. Intracranial aneurysms are found to be calcified in around 20% of the cases. Indeed, marginal calcifications first form after the intimal tear and are then followed by the formation of a sheet-like calcific plaque. In a study that involved 33 pediatric patients, aneurysms greater or equal to 10 millimeters were found to be calcified in contrast to ruptured aneurysms, implicating that calcified aneurysms tend to be more stable than uncalcified ones (14).

Interestingly mineralization of the lenticulostriate arteries has been associated with basal ganglia ischemic arterial strokes in the pediatric population (23). In a study done by Lingappa et.al, 22 out of 23 children (mean age of 11 months) with basal ganglia ischemic stroke were found to have mineralization of the lenticulostriate arteries on CT scan. In fact, 18 had mild head trauma prior to the onset of stroke whereas the remaining of the cohort had no predisposing factors with no demonstrable causes of vascular or soft tissue calcifications (23). In another study done by Gowda et.al, all children (mean age of 14 months) diagnosed with basal ganglia stroke had mineralization of the lenticulostriate arteries detected on CT scan (24). CT of brain showed sharply marginated, linear hyperdense lesions emerging vertically through the inferior part of the lentiform nucleus in all the infants. These lesions had attenuation values between 58 and 90 HU representing mineralization. The number of mineralized arteries varied from one to five on each side. The infarct was situated on one of the mineralization arteries (24).

Neoplastic

Brain calcifications are considered as important tool in the identification and evaluation of brain neoplasms. Indeed, the presence/absence of calcifications along with the patient's age and tumor location may help in the radiological identification of the neoplasm (4, 6).

Intra-axial

Astrocytomas include various intra-axial brain lesions and may calcify in up to 20% with calcifications reported in up to 25% of pilocytic astrocytoma cases. However, they are still considered as the most common intra-axial brain tumors to calcify because of their high incidence in the general population (4). Pilocytic xanthoastrocytoma affects adolescents and young adults with a median age of 17. It is usually superficially located and cortically based with an extensive involvement of the leptomeninges. It can appear as cystic lesion in most of the times with a mural nodule or as a solid mass. Calcifications may be seen in up to 40% of the cases and are usually associated with the solid form rather than cystic. Subependymal giant cell astrocytoma is usually seen in the first two decades of life. It is associated with TS with 15% of TS patients developing SEGA. They arise from the ventricular wall and the foramen of Monro and exhibit a well-demarcated round shape with a heterogenous pattern of calcifications if present. Whereas patients with pilocytic xanthoastrocytoma may present with seizure, patients with SEGA often present with hydrocephalus (14).

Oligodendrogliomas account around 5-7% of all hemispheric tumors in the general population. However, they are rare in the pediatric population and account for only 1% of pediatric brain tumors. Differentiation of oligodendrogliomas from oligoastrocytoma may be radiologically difficult and often requires genetic testing. They are usually located in up to 80% in the frontal and temporal lobes with no significant mass effect (14). Calcifications as well as other cystic lesions may be seen in oligodendrogliomas. Indeed, up to 40% of pediatric oligodendrogliomas may calcify whereas 90% oligodendrogliomas may calcify in adults (4, 14). Calcifications are associated with intra-tumoral vessels and may extend into the surrounding brain parenchyma (4) with a nodular and clumped pattern (6).

Gangliogliomas are less common than oligodendrogliomas in adults (4) whereas they are more common in the pediatric population and constitute 1-4% of all pediatric brain tumors. They are cortically based and are usually seen in the temporal lobe with a solid appearance in 43% of the cases and both solid and cystic appearance in 52% (14). They may calcify in up to 41% of the time (14) showing a mural calcified nodule (4).

Medulloblastoma is a highly malignant posterior fossa tumor. It is the most commonly seen in the posterior fossa and accounts for 38% of posterior fossa tumors in the pediatric population with a male predilection. Patients may present complaining from headache, vomiting and ataxia (14). On CT scan, medulloblastoma appear as a hyperdense lesion in the cerebellar vermis/hemisphere with tiny scattered dots or clumped (22) calcifications in up 22-29% of the cases (14) (Fig. 10).

Metastatic lesions may rarely calcify with the exception of metastatic lesions originating from the lung and breast as well as osteogenic sarcoma and mucinous adenocarcinoma. Calcifications may also develop secondary to radiation and chemotherapy (4).

Extra-axial

Meningiomas are extra-axial well-circumscribed lesions. Interestingly, they are more common in males in the pediatric population and are usually seen in atypical locations compared to their adult counterparts. Furthermore, pediatric meningiomas tend to exhibit a higher rate of recurrence, malignant subtypes and can be associated with neurofibromatosis (14). While Dinizio et. al have reported a 20% rate of calcification (14), Grech et. al state that calcifications may occur in up to 69% of all meningiomas (4). Calcifications may display a variety of patterns including sand-like, sunburst, rim and globular calcifications seen all over the tumor.

Craniopharyngiomas account for up to 50% of suprasellar tumors in children and may present as visual field disturbances, endocrine abnormalities involving the hypothalamic – pituitary axis, and headaches. Histologically, craniopharyngioma can be classified into adamantinomatous and squamous papillary with the former being the most common in children (14). Adamantinomatous

craniopharyngioma is seen on NCCT as cystic lesion with partial calcifications ranging from thin and circumferential to chunky appearance (14). Of note, craniopharyngiomas tend to calcify in up to 93% in the pediatric population (14) whereas they are less likely to calcify in adults (4) (Fig.11a).

Pineal tumors include a wide range of brain lesions ranging from benign low grade pineocytoma to highly aggressive pineoblastoma. Benign lesions tend to occur in adolescents and young adults whereas highly malignant lesions affect mostly children and adolescents. Pineocytoma often shows as well-circumscribed homogeneous lesion in contrast to pineoblastoma that shows an infiltrative mass with a heterogenous texture. Calcifications are commonly seen in up to 50% of all pineal tumors. In fact, calcifications occur in a peripheral fashion leading to the so-called exploded pattern of calcifications (14). According to Grech et.al, calcifications arising from the pineal gland itself often exhibit an exploded pattern whereas centrally located calcifications are produced by the pineal tumor (4) (Fig.11b).

Germ cell tumors can be subdivided into two categories: germinomatous germ cell tumors and non-germinomatous germ cell tumors. In male patients, 70% of cranial GGCT occur in the pineal gland area whereas in females, 75% of the lesions are supratentorial. Teratomas are most common lesions among the NGGCTs and show a heterogenous CT density due to its fat, soft tissue and osseous/cartilaginous content (14). Heterogenous calcifications along with germ cell layer elements in the pineal region of a young patient should raise suspicion of a possible underlying germ cell tumor, most commonly teratoma (4, 14) (Fig.11c).

Schwannomas, pituitary macroadenomas, dermoid and epidermoid tumors rarely calcify. However, lipomas often calcify and exhibit a characteristic egg-shell calcification pattern or central calcifications to a lesser extent (4).

Intraventricular

The most common intraventricular tumors to calcify are ependymomas, choroid plexus tumors, central neurocytoma, meningiomas and metastasis.

Intraventricular ependymomas exhibit calcifications in the form of dots or mass/rock-like (Fig.11d). In the posterior fossa, they are the most common to calcify as seen in up to 50%. Choroid plexus papilloma and carcinoma exhibit calcifications in 25% of cases, typically in the form of dots. In central neurocytomas, 50% of cases show calcifications varying from dots to large masses (25) (Fig.11e). Calcifications in intraventricular meningiomas have similar pattern to the extra-axial counterpart, seen in 50% of cases (6) (Fig.11f).

Metabolic/Endocrine

Generally, any disorder affecting calcium homeostasis may lead to brain calcifications including hypoparathyroidism and hyperparathyroidism (Fig.12) and hypothyroidism (Fig.13) to a lesser extent (14).

Hypoparathyroidism is characterized either by a state of low parathyroid hormone or end-organ resistance to PTH (14).

The exact epidemiology of hypoparathyroidism has been poorly studied. According to a population-based Rochester Epidemiology Project, the prevalence of hypoparathyroidism is estimated around 37 in 100,000 with post-surgical etiology being the most common. Common radiological features include osteosclerosis, calvarial thickening, soft tissue calcifications and hypoplastic dentition (26).

Brain calcifications affecting most notably the basal ganglia bilaterally and most commonly the globus pallidus. Calcifications may occur in the dentate nucleus, corona radiata, subcortical white matter and thalamus (26). Calcifications were thought to arise from a long-standing hyperphosphatemia (26) yet, the exact etiology remains unclear (14). Of note, similar symmetrical calcifications are noted as well in Fahr's disease and clinical and biochemical correlation is highly recommended (26).

Inflammatory

Systemic lupus erythematosus is a multifactorial disease believed to result from local vasculitis caused by antigen antibody complex deposition, thrombosis secondary to the interplay between antiphospholipid antibodies, platelets and blood vessel walls, and diffuse neuronal dysfunction. It occurs in up to 75% of patients with systemic lupus erythematosus yet remains challenging to early detect it (27). According to Raymond et. al (27) who studied 27 patients with cerebral lupus erythematosus, intracranial calcifications were noted either as isolated findings or along with brain atrophy or cerebral infarcts. Indeed, calcifications alone and calcifications with cerebral atrophy were noted in 11.11% of patients. Whereas, calcifications accompanied by both cerebral atrophy and ischemic lesions were noted in 7.4%. Calcifications were found to be symmetrical, bilateral involving most commonly the cerebellum followed by centrum semiovale, globus pallidus, putamen, head of caudate and thalamus (27).

Cerebral sarcoidosis may occur in 5-10% of sarcoidosis patients. Patients often present suffering from cranial neuropathy, cranial or multifocal neuropathy, and rarely multifocal hypertension (28). According to Lawrence et. al who presented 3 case reports of neurosarcoidosis, suprasellar calcifications were found in 1 out of 3 cases (29). According to Herring and Urich, hypothalamic and cerebellar calcifications were noted as well on autopsies (30).

Neurotoxicity

There are multiple causes of neurotoxicity in children including extrinsic toxins and insults such as lead poisoning and carbon monoxide (31). According to Reyes et. al, both cerebral and cerebellar calcifications were noted in 30 American adults with chronic lead exposure. Calcifications were described as punctiform, curvilinear, speck-like and diffuse. They were mostly found in the subcortical area, basal ganglia, vermis and cerebellum (32). According to Finelli et.al, calcifications were described at the level of the basal

ganglia, deep white matter, cerebral cortex and hippocampi (33).

Conclusion

Intracranial calcifications are common findings in NCCT scan of the head with NCCT being the modality of choice to characterize calcifications. They can be encountered in both pediatric and adult populations with a wide spectrum of presentations ranging from mild physiologic calcifications to brain neoplasms. As highlighted in this review, the patient's age, clinical findings, location and pattern of intracranial calcifications are essential clues for the proper diagnosis and management.

TEACHING POINT

Intracranial calcifications are common findings in non-contrast CT scan of the head. Nonetheless, a precise description of their radiological phenotype (size, location and shape) is essential in the diagnosis in combination with the patient's age and clinical presentation.

REFERENCES

- Livingston JH, Stivaros S, Warren D, Crow YJ. Intracranial calcification in childhood: a review of aetiologies and recognizable phenotypes. *Developmental Medicine & Child Neurology*. 2014 Jul;56(7):612-26. PMID: 24372060
- Deng H, Zheng W, Jankovic J. Genetics and molecular biology of brain calcification. *Ageing research reviews*. 2015 Jul 1;22:20-38. PMID: 25906927
- Yalcin A, Ceylan M, Bayraktutan OF, Sonkaya AR, Yuce I. Age and gender related prevalence of intracranial calcifications in CT imaging; data from 12,000 healthy subjects. *Journal of chemical neuroanatomy*. 2016 Dec 1;78:20-4. PMID: 274475519
- Grech R, Grech S, Mizzi A. Intracranial Calcifications: A Pictorial Review. *The neuroradiology journal*. 2012 Aug;25(4):427-51. PMID: 24029036
- Whitehead MT, Oh C, Raju A, Choudhri AF. Physiologic pineal region, choroid plexus, and dural calcifications in the first decade of life. *American Journal of Neuroradiology*. 2015 Mar 1;36(3):575-80. PMID: 25355815
- Kiroglu Y, Çalli C, Karabulut N, Öncel Ç. Intracranial calcifications on CT. *Diagnostic and Interventional Radiology*. 2010 Dec 1;16(4):263. PMID: 20027454
- Pilli VK, Behen ME, Hu J, Xuan Y, Janisse J, Chugani HT, Juhász C. Clinical and metabolic correlates of cerebral calcifications in Sturge-Weber syndrome. *Developmental Medicine & Child Neurology*. 2017 Sep;59(9):952-8. PMID: 28397986
- BOSE SC. A CASE REPORT OF STURGE WEBER SYNDROME. *University Journal of Medicine and Medical Specialities*. 2018 Apr 5;4(2). ISSN: 2455-2852

9. Zhang MN, Zou LP, Wang YY, Pang LY, Ma SF, Huang LL, Gao Y, Lu Q, Franz DN. Calcification in cerebral parenchyma affects pharmacoresistant epilepsy in tuberous sclerosis. *Seizure*. 2018 Aug 1;60:86-90. PMID: 29929111
10. Kresak JL, Walsh M. Neurofibromatosis: a review of NF1, NF2, and schwannomatosis. *Journal of pediatric genetics*. 2016 Jun;5(02):098-104. PMID: 27617150
11. Karikkineth AC, Scheibye-Knudsen M, Fivenson E, Croteau DL, Bohr VA. Cockayne syndrome: clinical features, model systems and pathways. *Ageing research reviews*. 2017 Jan 1;33:3-17. PMID: 27507608
12. Elitt CM, Volpe JJ. Degenerative disorders of the newborn. In *Volpe's Neurology of the Newborn 2018 Jan 1* (pp. 823-858). Elsevier. ISBN: 9780323531764
13. Savino E, Soavi C, Capatti E, Borrelli M, Vigna GB, Passaro A, Zuliani G. Bilateral strio-pallido-dentate calcinosis (Fahr's disease): report of seven cases and revision of literature. *BMC neurology*. 2016 Dec;16(1):165. PMID: 27608765
14. Dinizio AM, Vincent JK, Nickerson JP. Intracranial Calcifications in the Pediatric Age Group: An Imaging Review. *Journal of Pediatric Neuroradiology*. 2015 Sep;4(03):049-59. ISSN: 1309-6680
15. Patel DV, Holfels EM, Vogel NP, Boyer KM, Mets MB, Swisher CN, Roizen NJ, Stein LK, Stein MA, Hopkins J, Withers SE. Resolution of intracranial calcifications in infants with treated congenital toxoplasmosis. *Radiology*. 1996 May;199(2):433-40. PMID: 8668790
16. Aragao MD, van der Linden V, Brainer-Lima AM, Coeli RR, Rocha MA, da Silva PS, de Carvalho MD, van der Linden A, de Holanda AC, Valenca MM. Clinical features and neuroimaging (CT and MRI) findings in presumed Zika virus related congenital infection and microcephaly: retrospective case series study. *Bmj*. 2016 Apr 13;353:i1901. PMID: 27075009
17. Wasay M, Kheleani BA, Moolani MK, Zaheer J, Pui M, Hasan S, Muzaffar S, Bakshi R, Sarawari AR. Brain CT and MRI findings in 100 consecutive patients with intracranial tuberculoma. *Journal of Neuroimaging*. 2003 Jul;13(3):240-7. PMID: 12889171
18. Offiah CE, Naseer A. Spectrum of imaging appearances of intracranial cryptococcal infection in HIV/AIDS patients in the anti-retroviral therapy era. *Clinical radiology*. 2016 Jan 1;71(1):9-17. PMID: 26564776
19. Kim JM, Park KY, Bae JH, Han SH, Jeong HB, Jeong D. Intracranial Arterial Calcifications Can Reflect Cerebral Atherosclerosis Burden. *Journal of Clinical Neurology*. 2019 Jan 1;15(1):38-45. PMID: 30375758
20. Chen XY, Lam WW, Ng HK, Fan YH, Wong KS. The frequency and determinants of calcification in intracranial arteries in Chinese patients who underwent computed tomography examinations. *Cerebrovascular Diseases*. 2006;21(1-2):91-7. PMID: 16340183
21. Gezeran Y, Acik V, Çavu? G, Ökten AI, Bilgin E, Millet H, Olmaz B. Six different extremely calcified lesions of the brain: brain stones. *SpringerPlus*. 2016 Dec;5(1):1941. PMID: 27917338
22. Makariou E, Patsalides AD. Intracranial calcifications. *Applied Radiology*. 2009 Nov 1;38(11):48. ISSN: 0160-9963
23. Lingappa L, Varma RD, Siddaiahgari S, Konanki R. Mineralizing angiopathy with infantile basal ganglia stroke after minor trauma. *Developmental Medicine & Child Neurology*. 2014 Jan;56(1):78-84 PMID: 24102209
24. Gowda VK, Manjeri V, Srinivasan VM, Sajjan SV, Benakappa A. Mineralizing angiopathy with basal ganglia stroke after minor trauma: Case series including two familial cases. *Journal of Pediatric Neurosciences*. 2018 Oct 1;13(4):448 PMID:30937087
25. Crawford SC, Boyer RS, Harnsberger HR, Pollei SR, Smoker WR, Osborn AG. Disorders of histogenesis: the neurocutaneous syndromes. In *Seminars in ultrasound, CT, and MR 1988 Jun* (Vol. 9, No. 3, pp. 247-267). PMID: 3152491
26. John DR, Suthar PP. Radiological features of long-standing hypoparathyroidism. *Polish journal of radiology*. 2016;81:42. PMID: 26937260
27. Raymond AA, Zariah AA, Samad SA, Chin CN, Kong NC. Brain calcification in patients with cerebral lupus. *Lupus*. 1996 Apr;5(2):123-8. PMID: 8743125
28. Jachiet V, Lhote R, Rufat P, Pha M, Haroche J, Crozier S, Dupel-Potier C, Psimaras D, Amoura Z, Aubart FC. Clinical, imaging, and histological presentations and outcomes of stroke related to sarcoidosis. *Journal of neurology*. 2018 Oct 1;265(10):2333-41. PMID: 30109479
29. Lawrence WP, El Gammal T, Pool WH, Apter L. Radiological manifestations of neurosarcoidosis: report of three cases and review of literature. *Clinical radiology*. 1974 Jan 1;25(3):343-8. PMID: 4608759
30. Herring AB, Urich H. Sarcoidosis of the central nervous system. *Journal of the neurological sciences*. 1969 Nov 1;9(3):405-22. PMID: 5367038
31. Kontzialis M, Huisman TA. Toxic?Metabolic Neurologic Disorders in Children: A Neuroimaging Review. *Journal of Neuroimaging*. 2018 Nov;28(6):587-95. PMID: 30066477
32. Reyes PF, Gonzalez CF, Zalewska MK, Besarab A. Intracranial calcification in adults with chronic lead exposure. *American journal of roentgenology*. 1986 Feb 1;146(2):267-70. PMID: 3484574
33. Finelli PF, DiMario Jr FJ. Diagnostic approach in patients with symmetric imaging lesions of the deep gray nuclei. *The neurologist*. 2003 Sep 1;9(5):250-61. PMID: 12971836

FIGURES

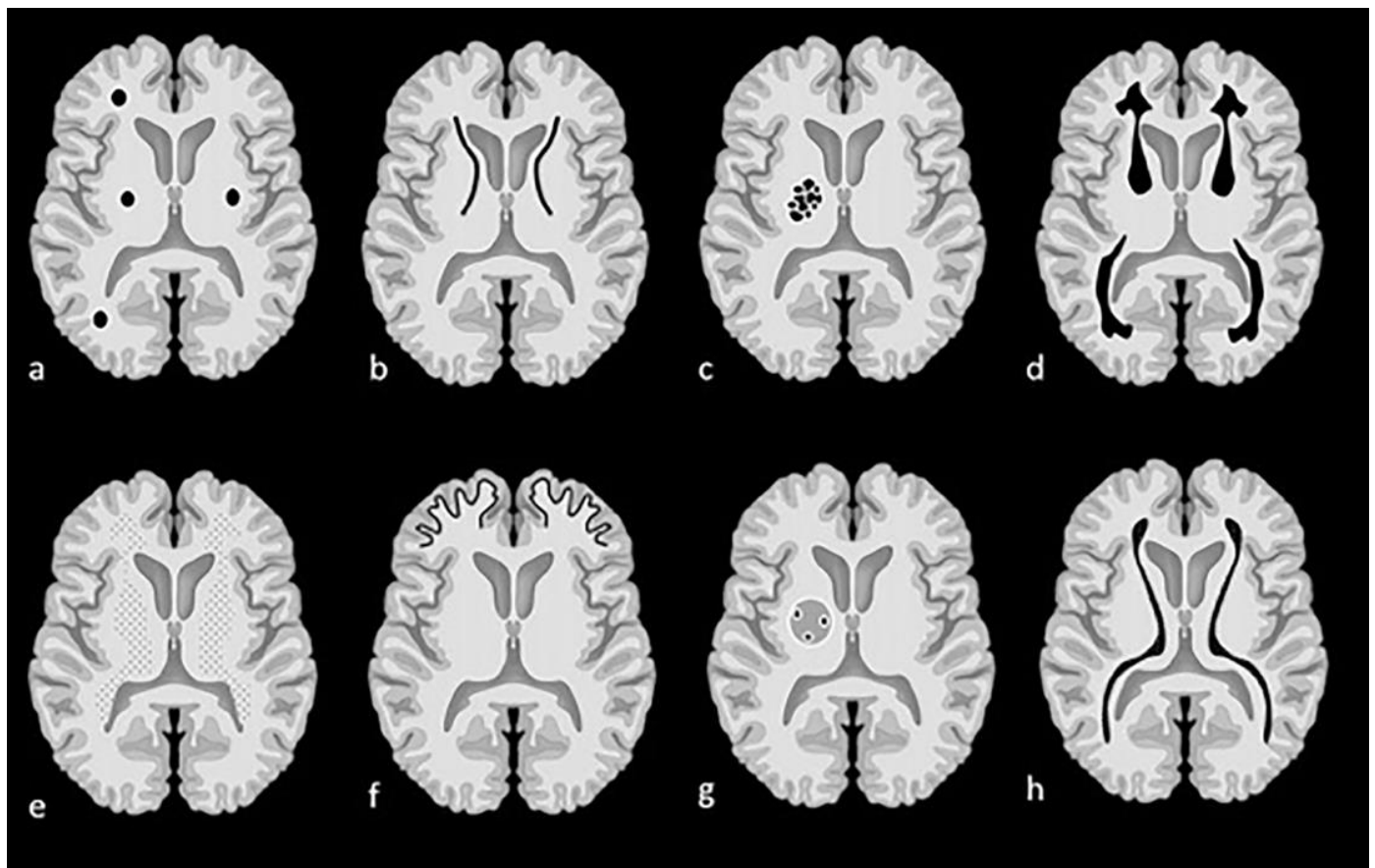


Figure 1: Examples of patterns of calcification and related terminology. (a) dots, (b) lines, (c) conglomerate or mass-like, (d) rock-like, (e) blush, (f) gyriform/band-like, (g) stippled (h) reticular.

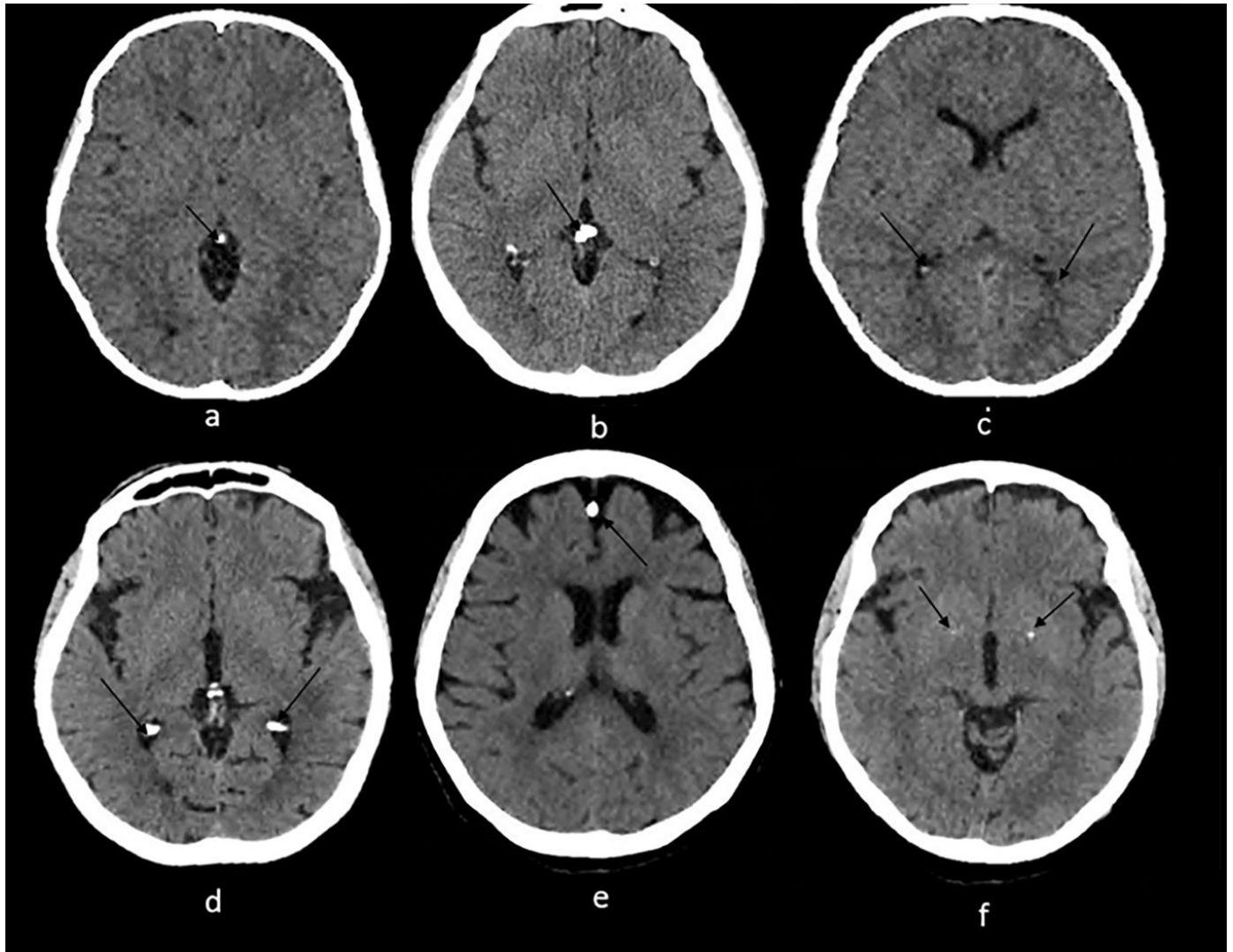


Figure 2: Technique: Axial non enhanced CT, 450 mAs, 120 kV, 0.8 mm slice thickness.

(a): 55-year-old female presenting to the ER post trauma.

Findings: Incidental dots of calcifications in the pineal gland (arrow).

(b) and (c): An 11-year-old male who presented to ER post MVA.

Findings: Incidental tiny dots (less than 1 cm) of calcifications with no soft tissue component in the pineal gland (2b) and choroid plexuses (2c) (arrows), a pattern suggestive of benign/ physiologic nature.

(d): 66-year-old male who presented to the ER for dizziness.

Findings: Incidental dots of calcifications in the bilateral choroid plexuses (arrows).

(e): 73-year-old male presenting to ER for high blood pressure and headache.

Findings: Incidental dot of calcification in anterior cerebral falx (arrow).

(f): 79-year-old male who presented to the ER post trauma.

Findings: Incidental isolated dots of basal ganglia calcifications (arrows).

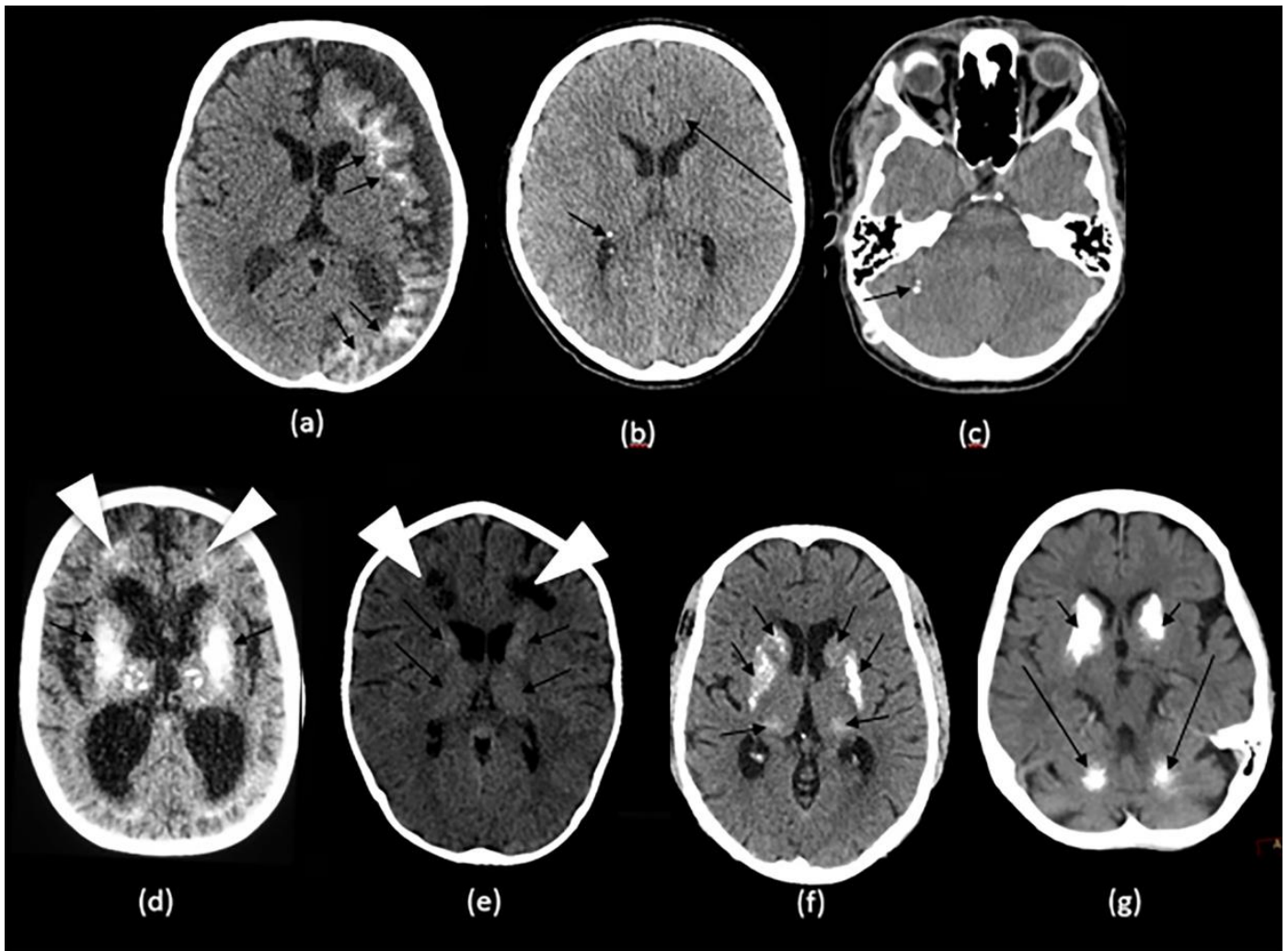


Figure 3: Technique: Axial non-enhanced CT, 450 mAs, 120 kV, 0.8 mm slice thickness

(a): 1-month-old infant boy with Sturge-Webber syndrome.

Findings: Diffuse gyral/subcortical white matter calcifications (arrows) with volume loss in the left cerebral hemisphere.

(b): 6-year-old boy with tuberous sclerosis.

Findings: Subependymal (short arrows) and subcortical tubers (long arrows), some of which are calcified.

(c): 40-year-old female with NF 2.

Findings: Right cerebellar hemisphere calcifications (arrow).

(d): 29-year-old male with Cockayne disease.

Findings: Bilateral conglomerate of calcifications in the globus pallidi, putamina, caudate nuclei and thalami (arrows) as well in the subcortical white matter (arrowheads). There is cerebral volume loss as seen by prominence of sulci and ventricles.

(e): 4-year-old boy with Krabbe disease.

Findings: Blush-like calcifications within the bilateral basal ganglia (arrows) including the thalami early in the course of the disease. In addition, there is decreased bifrontal peri-ventricular density from demyelination (arrowheads).

(f): 3-month-old infant girl with AGS.

Findings: Conglomerate of intracranial calcifications almost equally involving the basal ganglia (arrows) including the thalami. There is slight ex-vacuo dilatation of the ventricles and slight prominence of cerebral sulci secondary to volume loss.

(g): 42-year-old man with Fahr disease.

Findings: Conglomerate/mass like calcifications in the bilateral basal ganglia (short arrows), bilateral cerebellar white matter and dentate nuclei (long arrows).

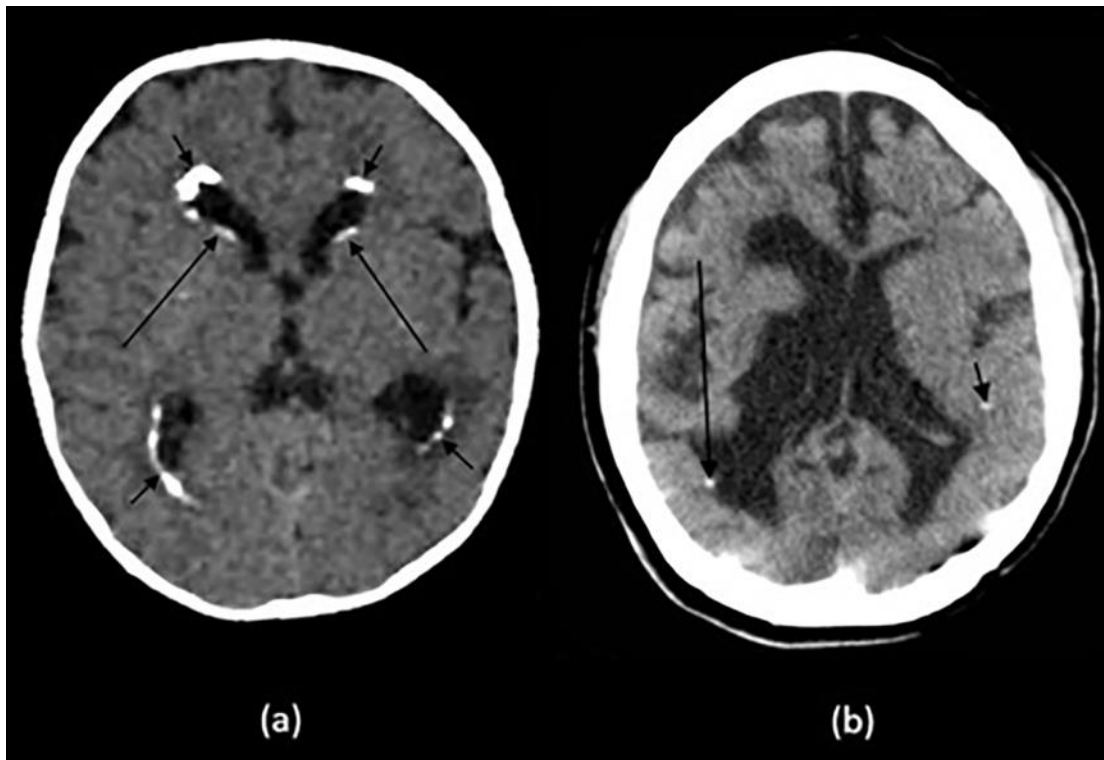


Figure 4: Technique: Axial non-enhanced CT, 450 mAs, 120 kV, 0.8 mm slice thickness.

(a): 10-month-old infant boy with seizures and neonatal CMV infection.

Findings: Reticular calcification pattern in the subependymal (long arrows) and periventricular region (short arrows) with mild ventriculomegaly.

(b): 21-year-old female with congenital toxoplasma infection.

Findings: Dots of calcification in the periventricular (long arrow) and subcortical (short arrow) regions with brain destruction, volume loss and ex-vacuo dilatation of the ventricles.



Figure 5 (left): 24-year-old male with previous HIV encephalitis.

Technique: Axial non-enhanced CT, 450 mAs, 120 kV, 0.8 mm slice thickness.

Findings: Coarse calcifications in the cerebral white matter (short arrows) and in the basal ganglia (long arrows).

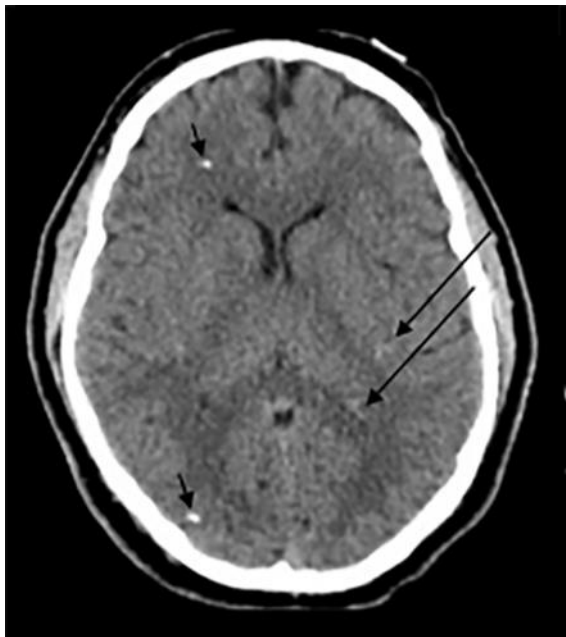


Figure 6 (left) : 33-year-old male with cysticercosis.

Technique: Axial non-enhanced CT, 450 mAs, 120 kV, 0.8 mm slice thickness.

Findings: Dots of calcifications in subependymal region (long arrow) and at gray to white matter interface (short arrows).

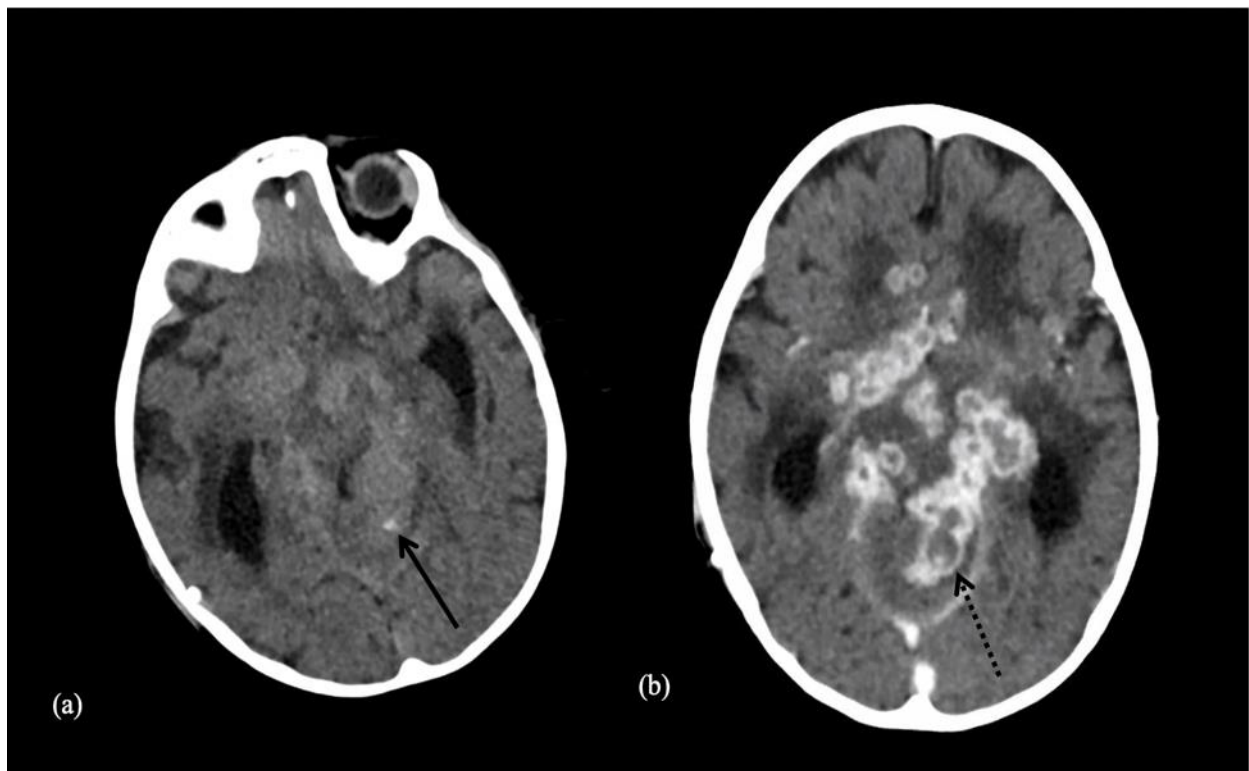


Figure 7: 9-year-old male patient with a tuberculoma.

Technique: Axial enhanced (b) and non-enhanced CT (a), 450 mAs, 120 kV, 0.8 mm slice thickness.

Findings: Tuberculoma with tiny calcification on both contrast and non-contrast enhanced CT scan. Both arrows show a central calcification within the tuberculoma.

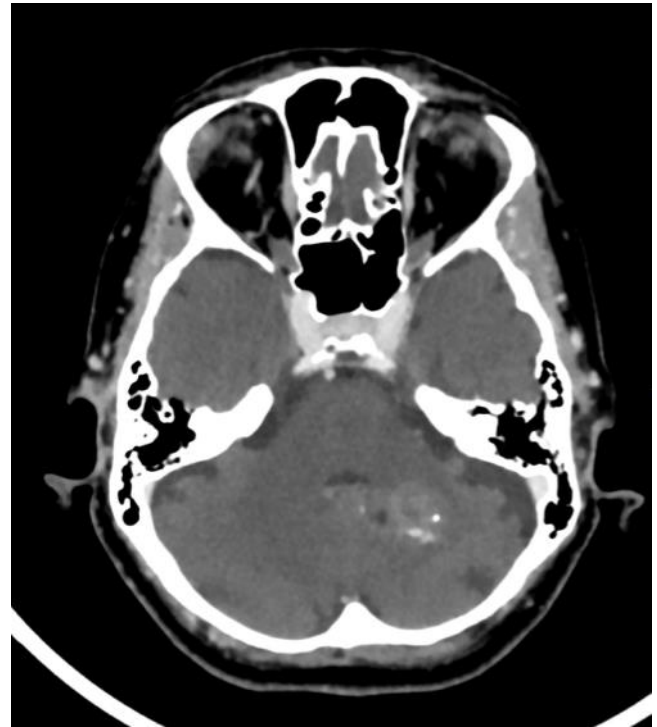


Figure 8: 68-year-old female patient presenting with bilateral internal carotid artery atherosclerosis.

Technique: Axial enhanced and non-enhanced CT, 450 mAs, 120 kV, 0.8 mm slice thickness.

Findings: Bilateral internal carotid artery atherosclerosis. Arrows show atherosclerotic calcifications.

Figure 9: 70-year-old female patient presenting with cavernous angioma.

Technique: Axial enhanced and non-enhanced CT, 450 mAs, 120 kV, 0.8 mm slice thickness.

Findings: Punctate calcification found in the cavernous angioma.

Figure 10 (right): 8-year-old male patient presenting with medulloblastoma.

Technique: Axial enhanced and non-enhanced CT, 450 mAs, 120 kV, 0.8 mm slice thickness.

Findings: Scattered and clumped calcifications.



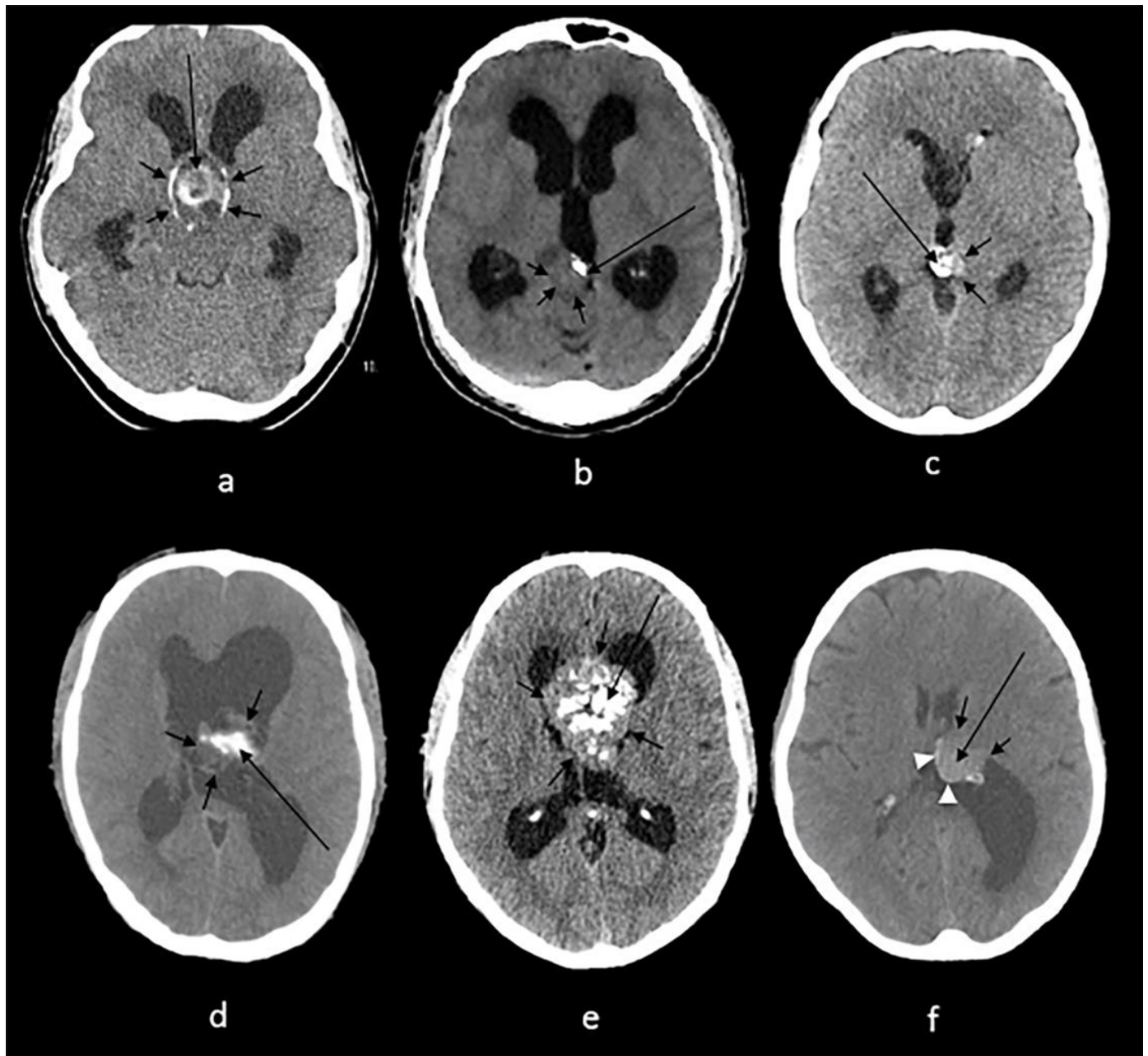


Figure 11: Technique: Axial non enhanced CT, 450 mAs, 120 kV, 0.8 mm slice thickness.

(a): 38-year-old female with craniopharyngioma.

Findings: A sellar/suprasellar mass-like (long arrow) and rim calcifications (short arrows) impinging on the foramen of Monro causing hydrocephalus.

(b): 20-year-old male with pineocytoma.

Findings: A mass in the pineal gland (short arrows) with peripheral calcification (long arrow).

(c): 13-year-old boy with pineal teratoma.

Findings: Conglomerate of dense calcifications (long arrow) inside the pineal mass (short arrows).

(d): 27-year-old male with intraventricular ependymoma.

Findings: An irregular mass centered in the body of left lateral ventricle (short arrows) containing dense mass-like calcifications (long arrow) with secondary enlargement of the lateral ventricles.

(e): 42-year-old male with central neurocytoma.

Findings: A mass in the septum pellucidum (short arrows) containing conglomerates of calcifications (long arrow), obstructing the foramen of Monro and causing hydrocephalus of lateral ventricles.

(f): 62-year-old female with intraventricular meningioma.

Findings: Interventricular meningioma centered in posterior body of left lateral ventricle (short arrows) showing internal blush-like calcifications (long arrow) and a rim of calcifications (arrowheads) with secondary enlargement of the left occipital horn.



Figure 12 (left): 29-year-old male with hyperparathyroidism.

Technique: Axial non enhanced CT, 450 mAs, 120 kV, 0.8 mm slice thickness.

Findings: Conglomerate of calcifications in the bilateral lentiform nuclei (long arrows) and in the bilateral thalami (short arrows).

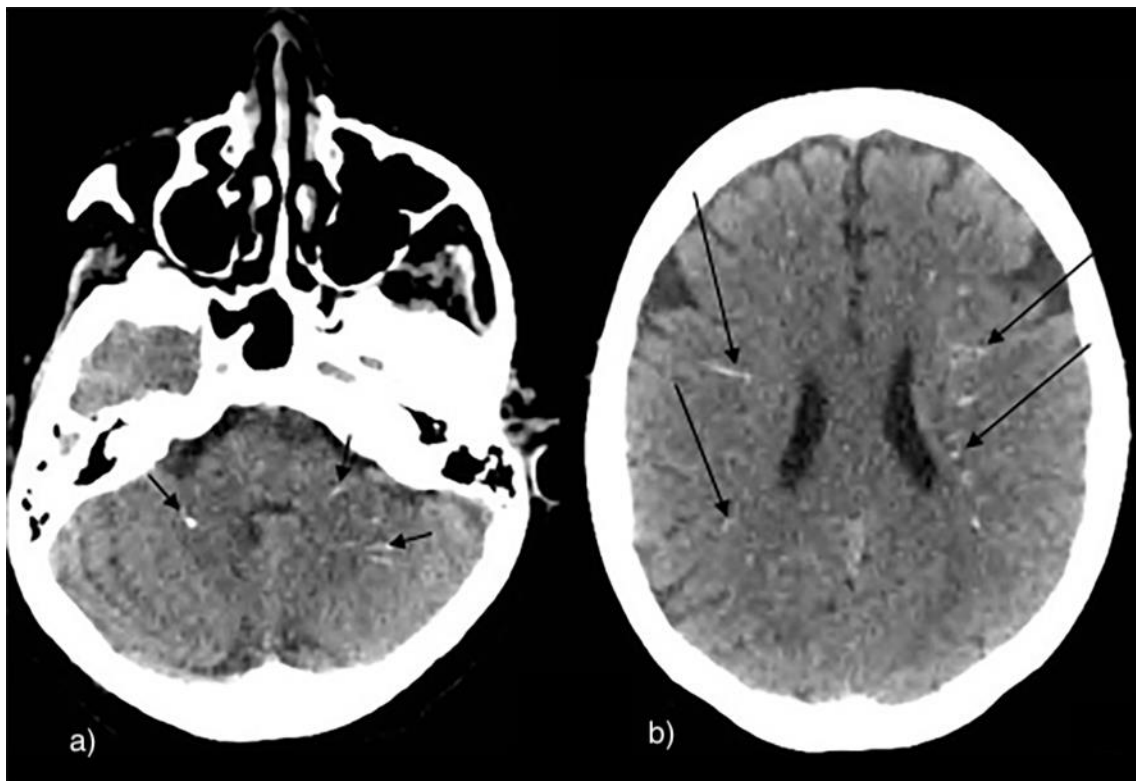
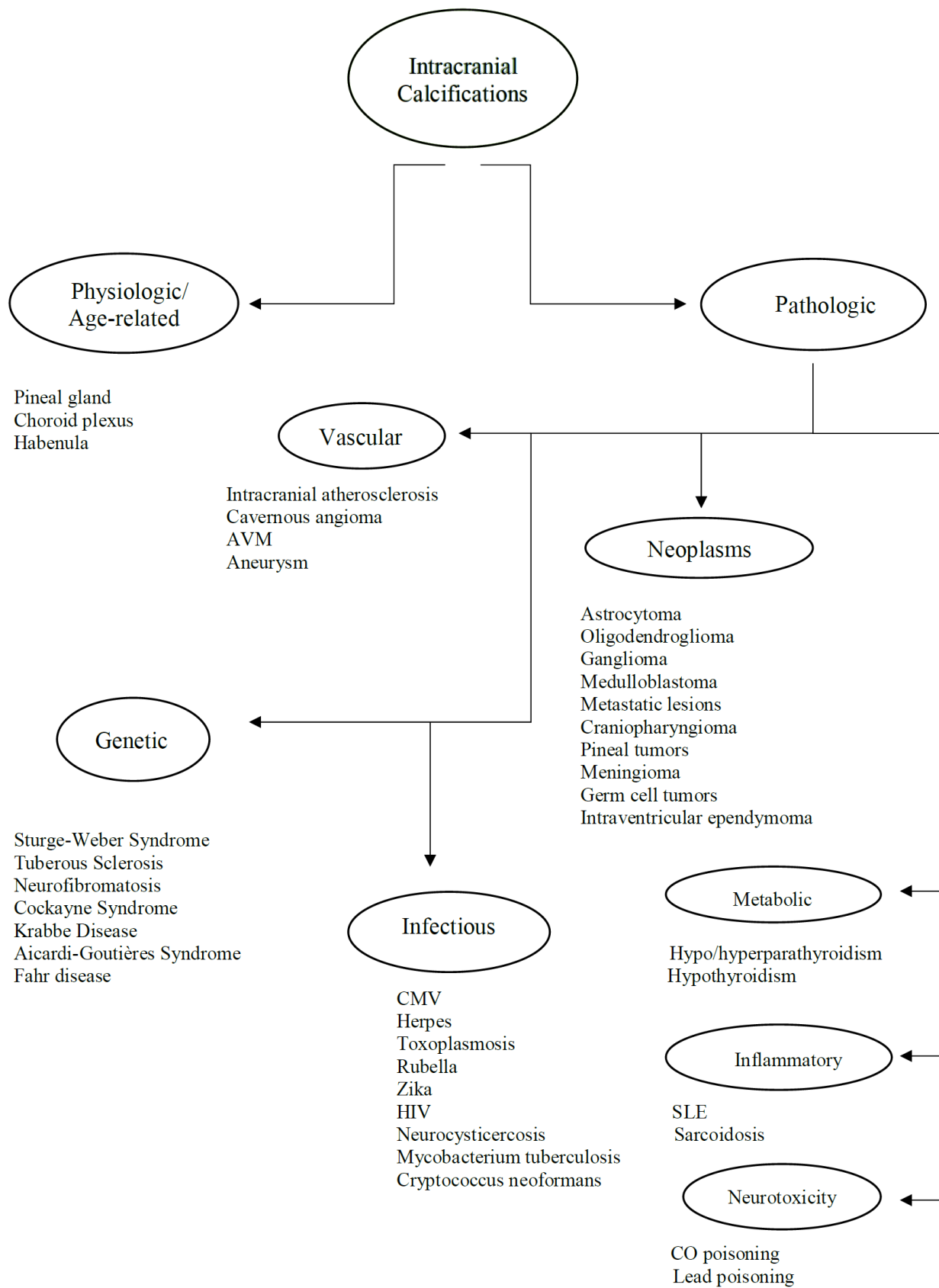


Figure 13: 63-year-old male with hypothyroidism.

Technique: Axial non-enhanced CT, 450 mAs, 120 kV, 0.8 mm slice thickness.

Findings: Multiple scattered small linear calcifications in the cerebellar (short arrows) and periventricular white matter (long arrows) bilaterally.



Journal of Radiology Case Reports

www.RadiologyCases.com

Table 1: Summary of intracranial calcifications

Intracranial Calcification	Etiologies	Location/Pattern
Physiologic/Age-Related Intracranial Calcifications		Pineal gland, choroid plexus, habenula, falx cerebri, tentorium cerebelli and basal ganglia. Coarse and compact, punctate, curvilinear.
Genetic / Developmental Disorders	Sturge-Weber syndrome	Tram track appearance, double-lined gyriform pattern.
	Tuberous sclerosis	Subcortical and subependymal tubers along the caudothalamic groove and atrium.
	Neurofibromatosis	Calcifications of the choroid plexus of the lateral ventricles and nodular calcifications of the cerebellum.
	Cockayne syndrome	Bilateral rock or spot calcifications at the level of the basal ganglia with or without gyral calcifications.
	Krabbe disease	Internal capsule and corona radiata,
	Aicardi-Goutières Syndrome	Symmetrical, spot-like calcifications at the level of the basal ganglia and deep white matter of both frontal and parietal lobes.
	Fahr disease	symmetrical, involving the caudate, putamen, globus pallidus, thalamus, deep cortex and dentate.
Congenital Infection	Cytomegalovirus	Thick chunky periventricular calcifications and faint punctate calcifications in the basal ganglia.
	Herpes	Scattered.
	Toxoplasmosis	Nodular periventricular and cortical calcifications and curvilinear in the thalamus and basal ganglia.
	Rubella	Basal ganglia and periventricular area.
	Zika	Punctate calcifications located between the cortex and subcortical white matter.
	Human Immunodeficiency Virus	Symmetrical in the basal ganglia and subcortical matter
Acquired infection	Neurocysticercosis	Eccentric calcified nodule within a peripherally calcified cyst in the brain parenchyma and subarachnoid space.
	Mycobacterium tuberculosis	Tuberculomas may calcify in the center giving the appearance of a pathognomonic target sign.
	Cryptococcus neoformans	Punctate calcifications in the brain parenchyma and leptomeninges.
Vascular		Scattered dots or stippled, symmetrical subcortical calcifications.
Intra-axial Neoplastic	Astrocytoma	Heterogeneous.
	Oligodendroglioma	Nodular and clumped.
	Ganglioglioma	Mural calcified nodule
	Medulloblastoma	Tiny scattered dots or clumped.
Extra-axial Neoplastic	Meningioma	Sand-like, sunburst, rim and globular.
	Craniopharyngioma	Thin and circumferential or chunky.
	Pineal tumors	Peripheral exploded pattern.
	Germ cell tumors	Heterogenous.
	Lipoma	Egg-shell or central.
Intraventricular	Ependymoma	Dots or mass/rock-like,
	Central neurocytoma	Dots to large masses.
Metabolic/Endocrine	Hypoparathyroidism	Basal ganglia, mainly
Inflammatory	Systemic lupus erythematosus	Cerebellum, mostly.
	Sarcoidosis	Suprasellar, hypothalamic and cerebellar areas.
Neurotoxicity	Lead and carbon monoxide	Punctiform, curvilinear, speck-like and diffuse.

Table 2: Summary of intracranial calcifications

ABBREVIATIONS

AGS = Aicardi-Goutières syndrome
 AIDS = Acquired immunodeficiency syndrome
 AVF = Arterio-venous fistula(s)
 AVM = Arterio-venous malformation(s)
 BGC = Basal ganglia calcification(s)
 CMV = Cytomegalovirus
 CNS = Central nervous system
 CS = Cockayne syndrome
 CT = Computed tomography
 GGCT = Germinomatous germ cell tumor(s)
 HIV = Human immunodeficiency virus
 IC = Intracranial calcification(s)
 MRI = Magnetic Resonance Imaging
 NCCT = Non-contrast computed tomography
 NF1 = Neurofibromatosis type 1
 NF2 = Neurofibromatosis type 2
 NGGCT = Non-germinomatous germ cell tumor(s)
 PTH = Parathyroid hormone
 SEGA = Subependymal giant cell astrocytoma
 SWB = Sturge-Weber syndrome
 TORCH = Toxoplasma, others, rubella, cytomegalovirus and herpes
 TS = Tuberous sclerosis

KEYWORDS

Intracranial calcifications; CT; Physiologic calcifications; Pathologic calcifications; Pediatric calcifications; Adult calcification

ACKNOWLEDGEMENTS

We would like to thank Dr. Mohammad Rawashdeh, Mr. Youssef Annous, Mr. Amer Traboulsi for their contribution in this review.

Online access

This publication is online available at:
www.radiologycases.com/index.php/radiologycases/article/view/3633

Peer discussion

Discuss this manuscript in our protected discussion forum at:
www.radiopolis.com/forums/JRCR

Interactivity

This publication is available as an interactive article with scroll, window/level, magnify and more features.
 Available online at www.RadiologyCases.com

Published by EduRad



www.EduRad.org